Multispectral scanning during endoscopy guides biopsy of dysplasia in Barrett's esophagus

Le Qiu[1,4], Douglas K. Pleskow[2], Ram Chuttani[2], Edward Vitkin[1,4], Jan Leyden[2], Nuri Ozden[2], Sara Itani[1], Lianyu Guo[1], Alana Sacks[2], Jeffrey D. Goldsmith[3], Mark D. Modell[1], Eugene B. Hanlon[1,5], Irving Itzkan[1,4], & Lev T. Perelman[1,4]

[1]Biomedical Imaging and Spectroscopy Laboratory and Department of Obstetrics, Gynecology and Reproductive Biology, [2]Division of Gastroenterology, Department of Medicine, [3]Department of Pathology, Harvard University and Beth Israel Deaconess Medical Center, Boston, Massachusetts, USA. [4]Department of Physics, Northeastern University, Boston, Massachusetts, USA. [5]Medical Research Service and Geriatric Research Education and Clinical Center, Department of Veterans Affairs, Bedford, Massachusetts, USA.

Correspondence should be addressed to L.T.P. (ltperel@bidmc.harvard.edu)

Supplementary Information

Nature Medicine: doi:10.1038/nm.2138

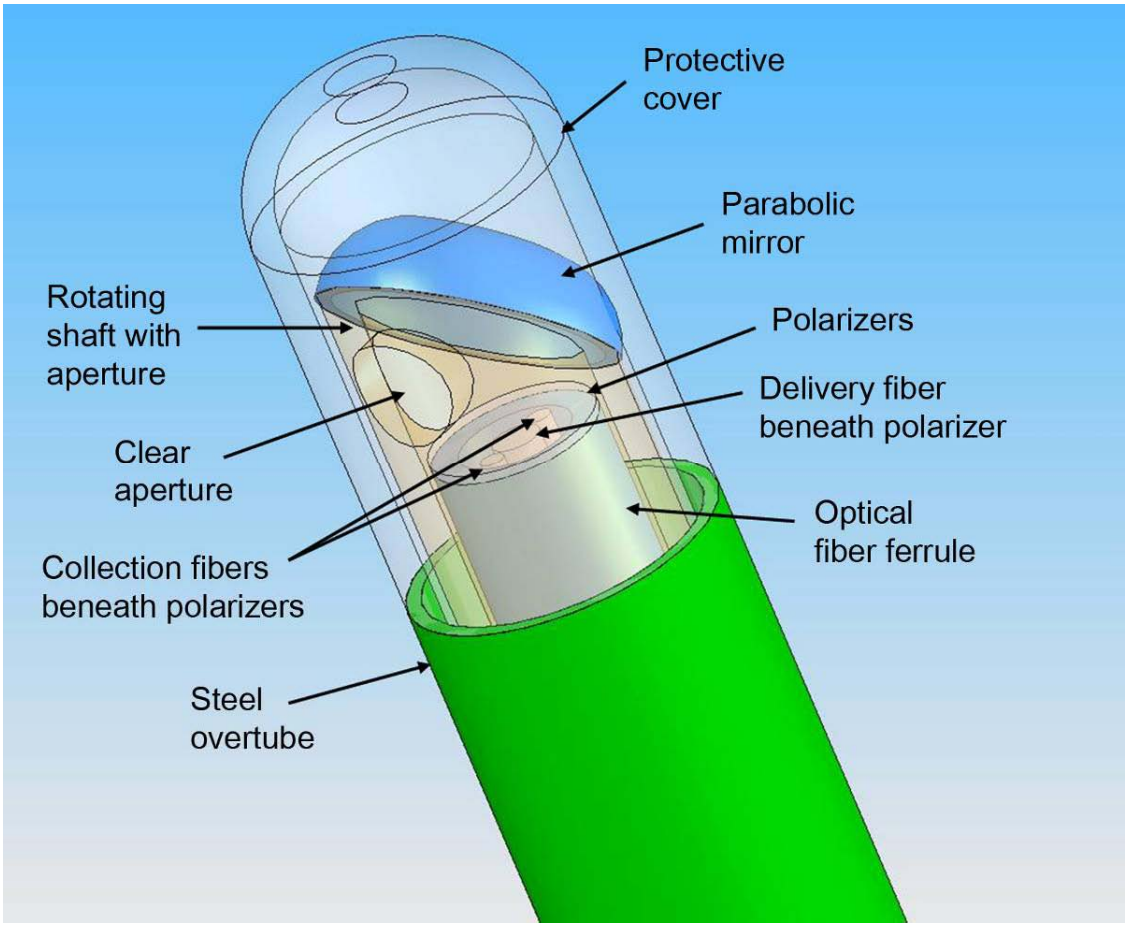

Supplementary Figure 1. Schematic of the EPSS scanning probe. Design detail of the probe tip showing key optical and mechanical components: parabolic mirror, polarizers, delivery and collection fibers, rotating shaft, steel overtube, fiber ferrule and protective cover.

Nature Medicine: doi:10.1038/nm.2138

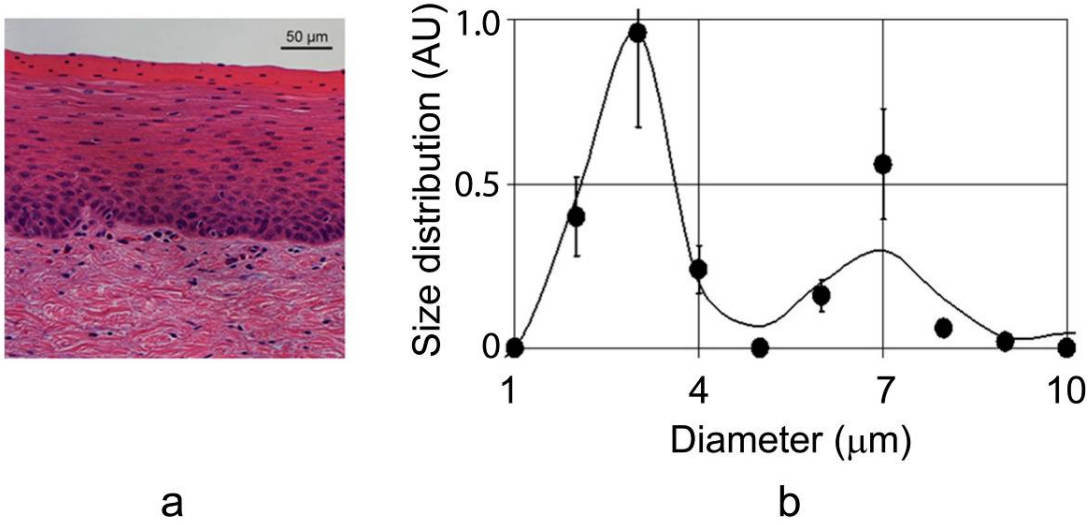

Supplementary Figure 2. Bovine lower-portion esophagus epithelium. (a) H&E staining. (b) Comparison of the nuclear size distributions extracted from the EPSS instrument measurements on intact epithelium (solid curve) and histological examination of the corresponding H&E stained sections (black dots).

Nature Medicine: doi:10.1038/nm.2138

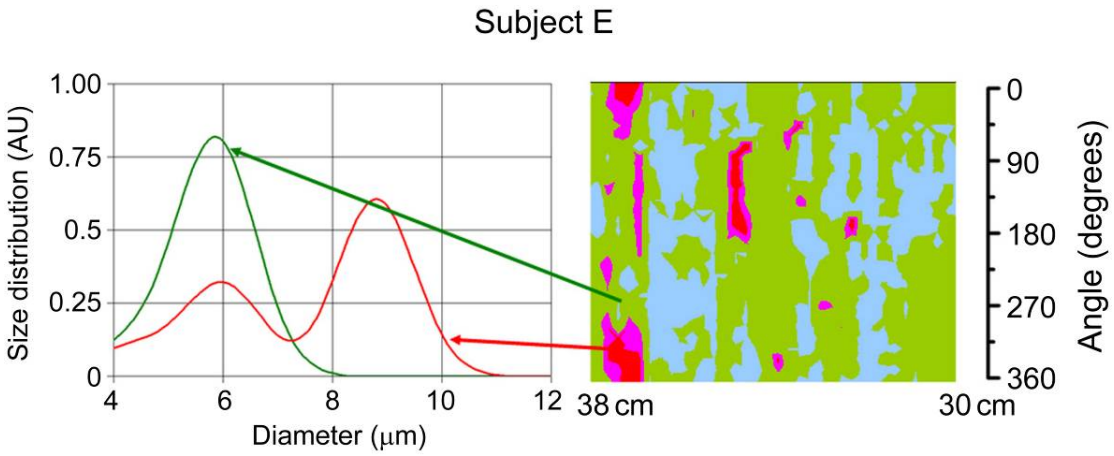

Supplementary Figure 3. Nuclear size distributions for one HGD site and one non-dysplastic site in Barrett's esophagus. Red and pink regions of the map indicate areas suspicious for dysplasia based on nuclear size distributions extracted from the backscattering spectra for each individual spatial location. Non-dysplastic Barrett's esophagus sites had nuclear size distributions centered about 5–6 μm diameter while sites marked as suspicious for dysplasia have nuclear size distributions with a main peak centered from 9 to 15 μm. The arrows indicate the specific locations on the esophageal surface from which the size distributions extracted from the EPSS data. (The map is from subject E).

Nature Medicine: doi:10.1038/nm.2138

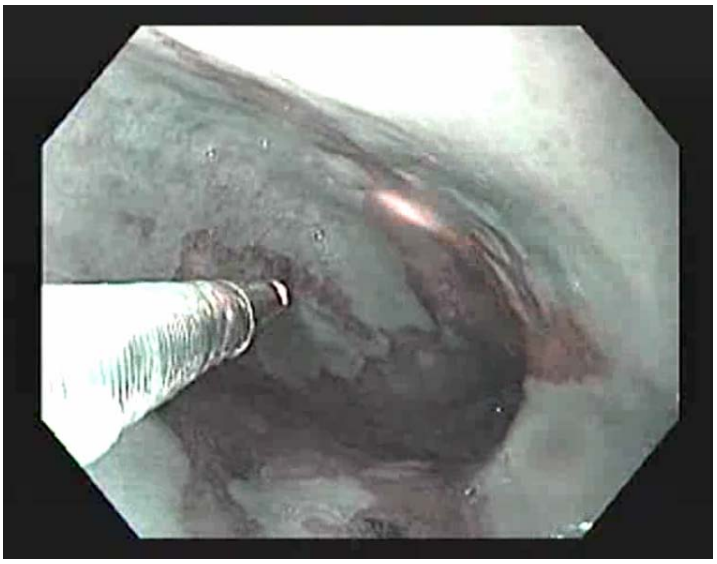

Supplementary Video 1. This video shows in real time the EPSS probe scanning a 2 cm section of esophagus during an endoscopy screening procedure. The regions of Barrett's esophagus, distributed in a diffuse pattern, appear darker in the video, which was acquired by the NBI of the endoscope.

Nature Medicine: doi:10.1038/nm.2138

Supplementary Methods

Algorithm and Software. Custom designed software, which can perform both scanning and data collection in imaging and single point modes, was developed within a National Instruments LabVIEW 8.5 interface. Video from the endoscope camera is acquired via the S-video output port of the video processor. It is overlaid with a pseudo-color map representing EPSS data. Currently the instrument collects 30 data points for each rotary scan (40 ms per spatial location) and performs ten steps during a linear scan (2 mm per step), collecting 300 data points for each 2 cm segment of Barrett's esophagus in 2 minutes, including repositioning time.

A simple algorithm used to distinguish non-dysplastic Barrett's esophagus from sites of HGD and LGD is described in **Methods**. To establish the physical basis for the above empirical analysis, we determined the contribution to the EPSS spectra of enlarged nuclei, a key histopathological feature of dysplasia. To determine the contribution of enlarged nuclei, we used an inverse algorithm to extract nuclear size distributions based on least–squares minimization, as described previously.[10,17,18]

The experimentally measured EPSS backscattering spectrum is a linear combination of the backscattering spectra of various subcellular organelles with different sizes and refractive indices. In order to extract the size distributions of these organelles, we express the experimental spectrum as a sum over organelles' diameters

Nature Medicine: doi:10.1038/nm.2138

$$S_m(\lambda) = \int_0^\infty I(\frac{\lambda}{\delta}, n, NA) N_m(\delta) d\delta + \varepsilon(\lambda) \qquad \text{(S.1)}$$

where $S_m(\lambda)$ is the normalized experimental spectrum collected with the EPSS probe having numerical aperture NA, $N_m(\delta)$ is the organelles' size distribution at site *m*, $I\left(\frac{\delta}{\lambda}, n, NA\right)$ is the Mie backscattering spectrum of a single scatterer with diameter δ and relative refractive index n, integrated over the NA of the probe, and $\varepsilon(\lambda)$ is the experimental noise. Then (S.1) can be written as a discreet sum over organelles' diameters

$$\hat{S}_m(\lambda) = \frac{C_R}{\lambda^4} + \sum_{\delta_R}^{\delta_{\max}} \hat{I}(\frac{\lambda}{\delta}, n, NA) \hat{N}_m(\delta) + \hat{E}(\lambda) \qquad \text{(S.2)}$$

where $\hat{N}_m(\delta) = N_m(\delta) d\delta$ is a discreet size distribution, $\hat{S}_m$ is the experimental spectrum measured at discrete wavelength points, $\hat{I}$ is the backscattering spectrum of a single scatterer, $\hat{E}$ is the experimental noise. Here the first term accounts for effects of Rayleigh scattering due to macromolecules and other scatterers smaller than δ_R, and $\delta_{\max}$ is the maximum biologically realistic nuclear size considered in the calculations. Equation (S.2) can be solved with the linear least squares with non-negativity constraints algorithm[19] using the methods described in our previous work.[10,17,18] Using this algorithm we can accurately reconstruct the size distributions of the nuclei present in the local illumination spot of the EPSS instrument.

This algorithm was tested on phantoms and has been used in experiments with freshly resected bovine esophagi (**Supplementary Fig. 2**) and clinical data analysis (**Supplementary Fig. 3**).

Nature Medicine: doi:10.1038/nm.2138

Animal Experiments. We checked the performance of the EPSS instrument in experiments using freshly resected bovine esophagi. The intact bovine esophagus was mounted vertically and an Olympus GIF-H180 gastroscope was inserted into the esophagus. The esophagus was scanned point-by-point and the EPSS data were recorded. We then performed histological examination of the sites where the EPSS data were collected.

The bovine esophageal tissues were fixed in 10% formalin for at least 24 hours, then processed and embedded in paraffin. Five micrometer thick serial sections were stained with hematoxylin and eosin (H&E) and photographed with a Zeiss Axio microscope.

The esophageal wall consists of four layers: mucosa, submucosa, muscularis propria and adventitia. Mucosa is the top layer and consists of epithelium, lamina propria and muscle tissue. As shown in **Supplementary Fig. 2a** the esophagus has stratified squamous epithelia to around 200 μm depth, whose purpose is to protect and lubricate during swallowing. Cells become flattened toward the surface. Lamina propria is a thin layer of connective tissue right under the epithelium layer, which contains collagen, reticular and sometimes elastic fibers. The muscularis mucosa, a thin band of longitudinal smooth muscle, extends throughout the entire esophagus.

As we can see in **Supplementary Fig. 2a**, the cells are very concentrated at the bottom of the epithelium layer where they originate. There, nuclei occupy almost the whole cell. The distance between cells increases as they move to the surface and the nuclei become elongated.

PLSS backscattering spectra depend mainly on the dimension of the scatterers along the direction of light propagation. Thus, short axis diameters

Nature Medicine: doi:10.1038/nm.2138

should contribute most in the measurements described here. The nuclei in the upper part of the epithelium have short axes of approximately 3 μm. In the bottom part of the epithelium, nuclear sizes vary from 5 μm to 8 μm and are randomly oriented. Comparing nuclear sizes in the H&E image with the EPSS result, we observed reasonable agreement (**Supplementary Fig. 2b**).

Clinical Measurements in Barrett's Esophagus Subjects. The subjects were administered conscious sedation. The subjects were placed in the left lateral decubitus position and an endoscope was introduced through the mouth and advanced under direct visualization until the second part of the duodenum was reached. Careful visualization of the upper gastrointestinal tract was performed.

A salmon colored mucosa distributed in a diffuse pattern, suggestive of Barrett's esophagus was found. Spectroscopy of the entire Barrett's segment was performed by scanning adjacent sections 2 cm in length with the EPSS probe. The endoscope tip was positioned and the probe was extended 2 cm beyond the endoscope tip, placing it at the boundary of a Barrett's esophagus region chosen for examination. One complete rotary scan of the esophageal wall was completed. The probe was withdrawn linearly 2 mm back into the endoscope tip and another rotary scan was completed. This was repeated until the entire 2 cm length of Barrett's esophagus had been scanned, then the endoscope tip was withdrawn 2 cm and the next length of Barrett's esophagus was examined. Linear positioning and rotary scanning of the endoscope tip added 2 minutes to the standard-of-care procedure for examining each 2 cm section of Barrett's esophagus. NBI available with the

Nature Medicine: doi:10.1038/nm.2138

Olympus EVIS EXERA II, CV 180 video controller was used simultaneously with spectroscopy recording and no interference from the endoscopic light source was observed in the PLSS spectra in the band from 600 nm to 800 nm. After EPSS scanning, four quadrant biopsies were performed every 2 centimeters, the current standard–of-care[14,15]. In addition, point spectroscopy followed by cold forceps biopsy for histology was performed at several individual locations of Barrett's esophagus.

The procedures were not difficult. The subjects tolerated the procedure well. There were no complications.

References

17. Itzkan, I., Qiu, L., Fang, H., Zaman, M.M., Vitkin, E., Ghiran, L.C., Salahuddin, S., Modell, M., Andersson, C., Kimerer, L.M., Cipolloni, P.B., Lim, K-H, Freedman, S.D., Bigio, I., Sachs, B.P., Hanlon, E.B. & Perelman, L.T. Confocal light absorption and scattering spectroscopic microscopy monitors organelles in live cells with no exogenous labels. *Proc. Natl. Acad. Sci. USA.* **104**, 17255-1760 (2007).
18. Fang, H., Qiu, L., Vitkin, E., Zaman, M.M., Andersson, C., Salahuddin, S., Kimerer, L.M., Cipolloni, P.B., Modell, M.D., Turner, B.S., Keates, S.E., Bigio, I., Itzkan, I., Freedman S.D., Bansil, R., Hanlon, E.B. & Perelman, L.T. Confocal light absorption and scattering spectroscopic microscopy. *Appl. Optics.* **46***,* 1760-1769 (2007).
19. Craig, I.J.D. & Brown, J.C. *Inverse Problems in Astronomy: A Guide to Inversion Strategies for Remotely Sensed Data* (A. Hilger, 1986).